Available online at www.sciencedirect.com

ScienceDirect

journal homepage: www.elsevier.com/locate/issn/15375110

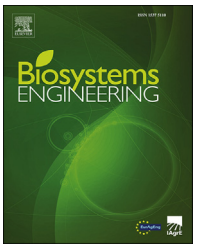

Special Issue: Biosystems and Metrology
Research Paper

Monitoring the hot-air drying process of organically grown apples (cv. Gala) using computer vision

Flavio Raponi, Roberto Moscetti, Swathi Sirisha Nallan Chakravartula, Marcello Fidaleo, Riccardo Massantini***

Department for Innovation in Biological, Agro-food and Forest Systems, University of Tuscia, Via S. Camillo de Lellis snc, 01100, Viterbo, Italy

ARTICLE INFO

Article history:
Published online xxx

Keywords:
Malus domestica B.
Image analysis
Dipping treatments
Vacuum impregnation
Smart drying
Area shrinkage

The feasibility of using a computer-vision (CV) system embedded in a hot-air dryer for non-destructive and real-time monitoring of the drying behaviour of organic apples was investigated in the present study. Apple cylinders were subjected to anti-browning treatments with different dipping solutions (water as control, trehalose (4% w/v) or trehalose + ascorbic acid (4% w/v and 1% w/v)) and dipping pressures (atmospheric, 101.3 kPa and sub-atmospheric pressure, 50 kPa) followed by drying at 60 °C to a final dry basis moisture content of 0.18 g g^{-1}. The CV system was used as an in-line process analytical technology (PAT) tool to capture images reflecting the physico-chemical changes during product drying coupled with in-line mass changes and off-line reference analyses. The spatial and colour changes from the image analysis described well the complex and non-homogenous nature of apple drying. The results of spatial changes allowed successful development of accurate linear prediction models for moisture content as a function of area shrinkage (on scaled variables) with excellent prediction capability (|BIAS| < 8.5 10^{-3}, RMSE < 0.04, Adj-R^2 ~ = 99%). Also, the CV system identified the differently pre-treated samples, particularly the dipping pressures as reflected by two linear models and their respective parameters. The obtained results demonstrate the versatile advantages of CV systems as an in-line tool for continuous, real-time monitoring of apples during drying. The insights from this study can provide a platform for applications of CV embedded 'Smart dryers' as an efficient monitoring and control system for industrial drying processes.

* *Corresponding author*. Tuscia University, Department for Innovation in Biological, Agro-food and Forest systems, Via S. Camillo De Lellis snc, 01100, Viterbo, Italy.
** *Corresponding author*. Tuscia University, Department for Innovation in Biological, Agro-food and Forest systems, Via S. Camillo De Lellis snc, 01100, Viterbo, Italy.
E-mail addresses: rmoscetti@unitus.it (R. Moscetti), massanti@unitus.it (R. Massantini).
https://doi.org/10.1016/j.biosystemseng.2021.07.005
1537-5110/

Please cite this article as: Raponi, F et al., Monitoring the hot-air drying process of organically grown apples (cv. Gala) using computer vision, *Biosystems Engineering*, https://doi.org/10.1016/j.biosystemseng.2021.07.005

Abbreviations

a*	Redness
AA	Ascorbic acid
Adj-R^2	Adjusted Coefficient of Determination
ANOVA	Analysis of Variance
a_w	Water Activity
b*	Yellowness
BI	Browning Index
C*	Chroma
CNT	Control
CSV	Comma-Separated-Values
CV	Computer vision
DNG	Digital Negative format
DP	Dipping Pressure
DS	Dipping Solution
DW	Dry Weight
h	Hue angle
L*	Lightness
MC_{db}	Moisture Content, dry basis
MCS	Monitor and Control Systems
P_{50}	Sub-atmospheric pressure
PAT	Process Analytical Technology
P_{atm}	Atmospheric pressure
PC	Principal Components
PCA	Principal Component Analysis
RGB	Red Green Blue
RMSE	Root Mean Square Error
SSC	Soluble Solids Content
t_0	Initial Time of drying
TA	Titratable Acidity
t_f	Final Time of drying
TR	Trehalose

1. Introduction

Consumers are becoming more critical and demanding in their food choices with a strong trend in the consumption of fruits and vegetables, functional foods (Kearney, 2010) as well as organic foods (Janssen, 2018). With the European policies pushing towards sustainable agriculture and food production with long-term goals to be achieved by 2050, the industry must also meet the population needs and consumer expectations in a cost-effective way.

As such, preservation strategies that enhance food stability have an enormous impact on the globalised market to reduce food losses and directly affect the production and distribution costs (Moscetti et al., 2017). In this context, drying is an effective method for improving the storability of perishable produce by inhibiting microbial spoilage to a great extent by lowering the water activity (a_w) (Maltini et al., 2003) as well as reducing supply chain costs by enabling ambient storage, reducing the size and mass of the products (Moscetti et al., 2018a).

Food drying in industry is largely carried out by convection based hot-air dryers due to their relative simplicity of use (Ngamwonglumlert & Devahastin, 2017) and they occupy > 85% of the market. However, these dryers are frequently criticised for (i) because they require extended heat exposure leading to non-uniformity and undesirable changes in product quality, particularly in uncontrolled processes leading to under and/or over-drying (Defraeye, 2014; Raponi et al., 2017) and (ii) their energy consumption consists of up to 25% of the total energy demand leading to higher fossil fuel usage (Defraeye, 2014). To overcome these drawbacks, studies have been carried out over the years in order to improve drying in terms of (i) energy efficiency, through the implementation of heat recovery systems (Barbosa de Lima et al., 2015; Kemp, 2005), (ii) sustainability, benefiting from the free and renewable energy sources (Basunia & Abe, 2001; El-Sebaii & Shalaby, 2012; Koyuncu, 2006; Tunde-Akintunde, 2011); (iii) quality of final product, testing various pre-processing of products; and (iv) quality of process and product, embedding process monitor and control systems (MCS) (Lukinac et al., 2013; Mujumdar & Law, 2010; Winiczenko et al., 2018). Of these, the use of MCS within dryers can allow for uninterrupted flow and end point determination during the process by real-time measurements (van den Berg et al., 2013).

Of the various embedded MCS processes investigated, one of the emerging and perhaps most promising technologies is 'smart drying', a strategy based on the process analytical technologies (PAT) (Moscetti et al., 2018a). PAT uses innovative and reliable resources from different sectors like visible and near-infrared spectroscopy (Moscetti et al., 2019; Moscetti et al., 2018a; Pomerantsev & Ye, 2012), biomimetics (i.e., electronic nose, tongue, and mucosa), computer vision and imaging systems (Moscetti, Sturm, et al., 2018; Raponi et al., 2017; Xu et al., 2017; Yaseen et al., 2017) combined with chemometrics and machine learning techniques in general (Su et al., 2015; Sun et al., 2018). Among the various PAT tools, computer vision (CV) is increasingly been adapted to meet demands of the food industry in recent years due to its accuracy and consistency in product quality evaluation (Fernández et al., 2005; Raponi et al., 2017). Also, these systems can be applied for in-/at-/on-line or off-line measurements to effectively monitor the key physico-chemical characteristics like the visual perception and appearance for consumers (Lawless, 1999) as well as morphological changes in the product (Aghbashlo et al., 2014; Sampson et al., 2014).

This approach is of industrial relevance, specifically in case of fruits such as apple which are of commercial interest owing to their increasing consumption as snacks, chips, and their use as intermediate products in integral breakfasts (Vega-Gálvez et al., 2012). In fact, apples are frequently become discoloured due to enzymatic browning and/or occurrence of Maillard's reaction during drying. Anti-browning pre-treatments using additives such as acidulants (e.g., ascorbic acid, citric acid), sugars (e.g., mono-, di-saccharides) and antioxidants (Aktas et al., 2007; Singh et al., 2015) by conventional dipping or by use of vacuum impregnation at sub-atmospheric pressures have been shown not only to enrich plant tissues with additives/ingredients but also to improve overall product quality (Neri et al., 2016a).

Although the use of different pre-treatments in apple drying has been widely studied in literature, to the best of our knowledge there is little insight available as to the feasibility of CV as a PAT tool for monitoring the drying of pre-treated organic apple cylinders in the smart drying

Please cite this article as: Raponi, F et al., Monitoring the hot-air drying process of organically grown apples (cv. Gala) using computer vision, *Biosystems Engineering*, https://doi.org/10.1016/j.biosystemseng.2021.07.005

sector. Therefore, the objective of this research was to evaluate the use of computer vision system as an in-line tool for (i) non-destructive real-time monitoring of drying behaviour, morphological and colour changes in organic apple cylinders and (ii) flexibility and robustness of the CV-based moisture prediction models when applied to the drying of samples subjected to common industrial processes such as chemical and/or physical pre-treatments.

2. Materials and methods

2.1. Sample preparation

Apples (*Malus domestica* B. var. Gala) grown organically were purchased from a local trader (Biobox srl, Viterbo, Italy) and immediately stored at 2 ± 1 °C until further processing. Sound apples with uniform size and same ripening stage were selected and tempered to room temperature for 15 h before use in the experiments. Apples were washed and cut into slices (5-mm thick) using an electric stainless-steel food slicer (mod. 380, ALA2000, Treviso, Italy) (Fig. 1a) for which the core and peel were removed. Subsequently, apple cylinders of approximately 3.5 ± 0.1 g and a diameter of 23 ± 1 mm were obtained using an iron steel pastry mould. The shape and dimensions were chosen to have cylinders representative of bite-sized snacks. Samples were visually assessed for quality and only cylinders free from decay and/or blemishes were used in the experimentation.

2.2. Smart-enabled prototype dryer set-up

The prototype dryer consisted of (i) a temperature-controlled centrifugal fan dryer (mod. Biosec domus B5, Tauro Essicatori srl, Vicenza, Italy) which horizontally blew air into the 26.50 L drying chamber (~240 × 240 × 460 mm) through a 150 mm duct, (ii) a computer vision (CV) setup placed on the top and (iii) a digital balance (mod. HT1500, NHU, Germany) placed on the base of the drying chamber, respectively (Fig. 2).

In detail, the CV setup consisted of (i) a CMOS camera (mod. EOS 400D, Canon, Japan), (ii) an illumination source, (iii) a DC 12V electrical circuit breaker equipped with a relay module (mod. SRD T73, Ningbo Songle Relay, China), (iv) a single-board computer (mod. Raspberry Pi B+, Raspberry Pi Foundation, UK) used as a monitoring system and (v) a 300-W DC power supply (mod. 300XX, Codegen Technology, China). The

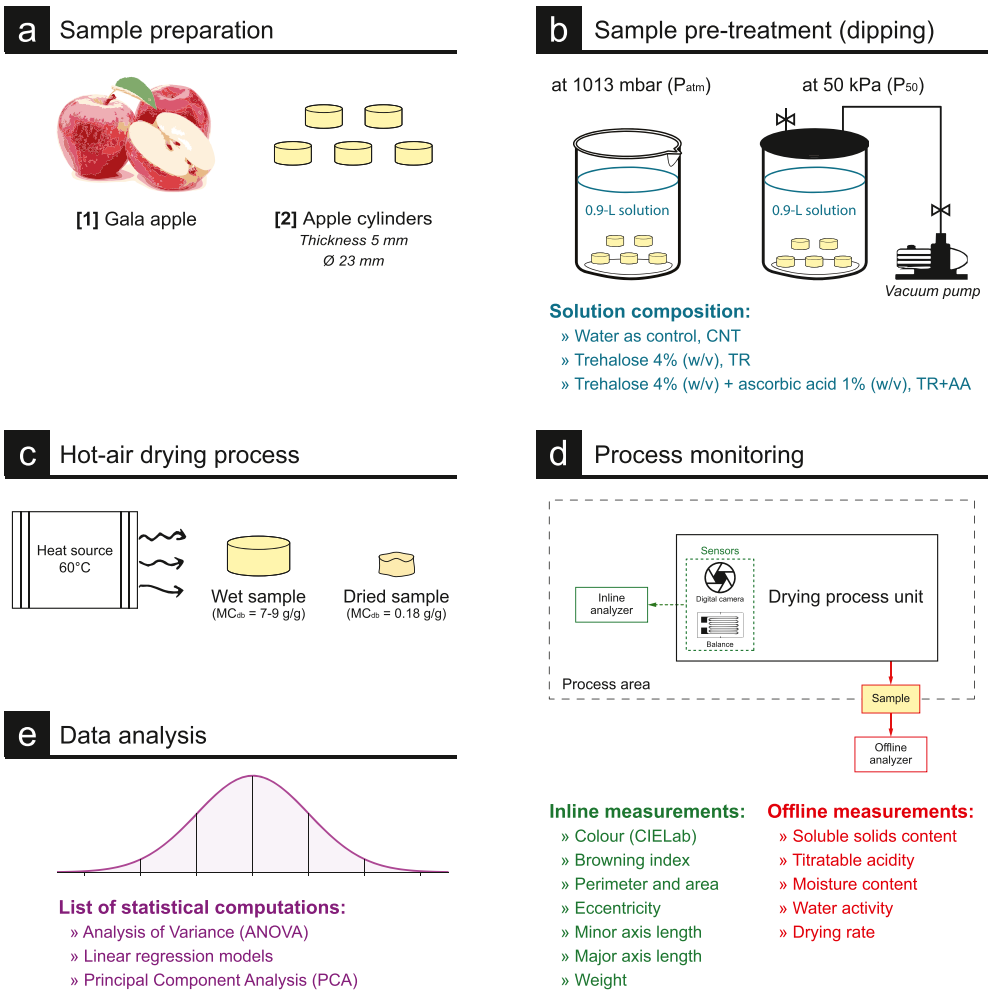

Fig. 1 – Simplified step-by-step representation of (a) sample preparation, (b) dipping treatments, (c) hot-air drying process, (d) process monitoring and (e) data analysis procedures.

Please cite this article as: Raponi, F et al., Monitoring the hot-air drying process of organically grown apples (cv. Gala) using computer vision, *Biosystems Engineering*, https://doi.org/10.1016/j.biosystemseng.2021.07.005

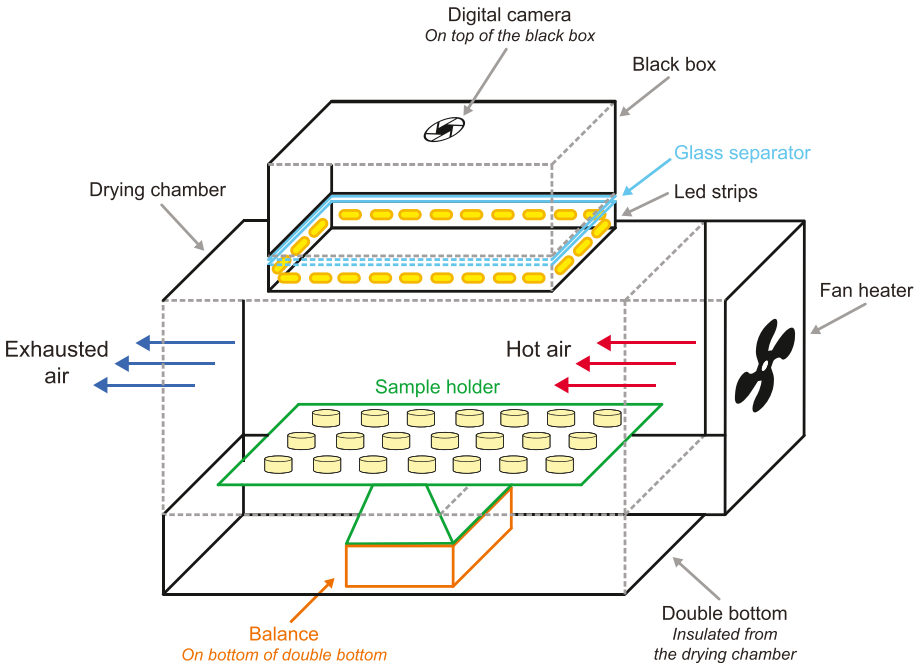

Fig. 2 – Schematic representation of the smart enabled prototype convection-based cabinet dryer.

digital camera was mounted inside a black box, insulated from external light, and placed on the top of the dryer chamber. The illumination source consisted of four light-emitting diode strips (colour temperature of 4200 K) arranged along the top side of the box to improve the intensity and uniformity of the light along the field of view, and response of the camera.

The monitoring system was programmed in Python 3.7 (Python Software Foundation, USA), using the Jupyter notebook (Perez & Granger, 2015) as front-end. It allowed (i) to turn on/off the illumination source through the electric circuit breaker, (ii) to scan images of the top surface area of the product in sync with the illumination source and (iii) to weigh the samples.

2.3. *Sample pre-treatments*

A replicated full-factorial experiment with two factors (dipping solution, or DS, and dipping pressure, DP) was used to test the effect of the pre-treatments. For the factor DS, three dipping solutions were tested (Fig. 1b): (i) water as control (CNT); (ii) trehalose 4% w/v (TR); and (iii) trehalose 4% w/v with ascorbic acid 1% w/v (TR+AA). Ascorbic acid was used for its well-known inhibition effect towards polyphenol oxidase (Albanese et al., 2007; El-Shimi, 1993). Whereas, trehalose, a natural disaccharide generally recognised as safe (Megarry et al., 2011) was used for its known ability to preserve tissue structure, prevent protein denaturation as well as reducing non-enzymatic browning occurrence (Aktas et al., 2007; Albanese et al., 2007).

As for the factor DP, two different dipping pressures were tested: (i) atmospheric pressure at 101.3 kPa (P_{atm}) as conventional dipping pressure and (ii) sub-atmospheric pressure (or vacuum impregnation) at 50 kPa (P_{50}), for its higher potential in stabilising and embedding vegetal tissues with functional components/solutes (Neri et al., 2016a).

All the treatments were carried out at ambient temperature on 50 cylinders of apple (~180 g) with a product: solution ratio of 1:5 (w/v). The P_{50} treatment was carried out using a laboratory-scale vacuum equipment composed of a vacuum chamber (maximum capacity of 5 L), connected to a vacuum pump (KNF N 840.3 FT.18, Trenton, USA) (Fig. 1b). The samples were subjected to a sub-atmospheric pressure of 50 kPa for 0.25 min, and then equilibrated at atmospheric pressure for 5 min. Whereas P_{atm} samples were submerged in dipping solutions for a total of 5.25 min. After the pre-treatment, samples were drained off using absorbent paper and left to dry at ambient temperature for 3 min.

Each treatment, obtained as a combination of DS and DP, was replicated two times, thus producing a total of 12 batches of apple cylinders. Within each batch, 50 apple cylinders were randomly subjected to each pre-treatment in duplicates. Of these, 25 cylinders were selected and immediately subjected to hot-air drying process with in-line measurement (section 2.4); whilst the other 25 cylinders were used as fresh samples for off-line reference analysis (section 2.5).

2.4. *Hot-air drying process with inline measurement*

A hot-air drying experiment was performed at 60 °C (Fig. 1c) based on pre-screening tests of temperatures in the range 40–60 °C. The selected temperature was chosen because it gave better colorimetric parameters among the tested temperatures as that temperature is also extensively used in apple drying (Sacilik & Elicin, 2006; Simal et al., 1997; Velić et al., 2004). Twenty-five apple cylinders from each batch of DS and DP treatment combinations were dried to a final dry-basis moisture content (MC_{db}) of approx. 0.18 g g^{-1}.

Please cite this article as: Raponi, F et al., Monitoring the hot-air drying process of organically grown apples (cv. Gala) using computer vision, *Biosystems Engineering*, https://doi.org/10.1016/j.biosystemseng.2021.07.005

For the in-line measurements, the sample mass and image were acquired every 5 min for the entire drying period. The sample weight was stored as Comma-Separated-Values (CSV) file, whilst sample images were acquired in raw digital negative (DNG) image format. The resolution of the digital image was 2592 × 3888 pixels (240 dpi) and its colour intensity resolution was 24 bits, corresponding to 8 bits per RGB channel.

2.5. Data post-processing and features extraction

The changes in dry-basis moisture content (MC_{db}) during drying were computed by combining data from (i) the fresh mass of samples before drying, (ii) their changes in mass collected in-line during drying and (iii) the off-line analysis of moisture content after drying. Moisture data was relativised for modelling by applying a min–max data normalisation, i.e., scaling values of moisture content to a common 0-1 scale, without distorting differences among the treatments. Additionally, both overall drying rate and punctual drying rate were computed and expressed as rate of moisture removed per gram of dry matter per hour (i.e., g [H_2O] g^{-1} [DW] h^{-1}).

The camera was calibrated using a Colorchecker Passport target (X-Rite Ltd., UK). Subsequently, each DNG image was colour corrected by applying the camera profile through the Camera Raw 6.0 software (Adobe Systems Inc., San Jose, CA, USA) and then saved as raw tagged image file format (TIFF).

Image segmentation for features extraction (i.e., colour and spatial data extraction) was performed as a last stage of the image post-processing, using a script written in Python 3.7.0 coupled with the OpenCV 3.4.1 library, with the aim of separating the true image of each sample (i.e., foreground) from the background (i.e., non-sample data). For the intended purpose, the Otsu's binarisation method was used as clustering-based image thresholding.

The Python script was also used to extract the average colour of each apple cylinder. Specifically, the 'cvtColor()' function of the OpenCV library was applied for the sRGB-to-CIELab colour space conversion. Thus, results were expressed in terms of lightness (L*), redness (a*), yellowness (b*), hue angle (h) and chroma (C*) (Moscetti et al., 2013). In addition, the browning index (BI) was computed as the most common descriptor of browning development in foods (Pathare et al., 2013) according to Eq. (1):

$$BI = 100 * \frac{(X - 0.31)}{0.172} \quad (1)$$

where X was computed according to Eq. (2):

$$X = \frac{(a^* + 1.75L^*) * a^*}{(5.645L^* + a^* - 3.012b^*)} \quad (2)$$

Spatial features such as major and minor axis lengths (mm), perimeter (mm), surface area (mm^2) and eccentricity of apple cylinders were extracted using Matlab 2018b coupled with the 'Image Processing' toolbox (MathWorks, CA, USA). Measurements were performed using the 'regionprops()' function. Axis lengths were measured as major and minor axis of the ellipse with the same normalised second central moments (i.e., rotational inertia) in the cylinder region. Perimeter and surface area were acquired by counting the number of pixels. Eccentricity was computed as the ratio of the distance between the foci of the ellipse and its major axis length. Size and shape parameters were converted from pixel to metric unit (mm) by scanning the reference embedded in the Colorchecker Passport target (X-Rite Ltd., UK). Finally, the relative area shrinkage was computed by dividing each measurement over time by the initial value (i.e., surface area in pixels).

2.6. Off-line measurements

The off-line measurements were carried out on 25 fresh and dried apple cylinders from each batch and each treatment combination. The samples were evaluated for the effect of pre-treatments on the general quality parameters in relation to the changes observed by in-line analysis.

Moisture content was carried out following AOAC 934.06 official method using a hot-air oven (mod. U 40, Memmert, Germany) and results were expressed on a dry basis (MC_{db}). The water activity (a_w) was determined with a water activity meter (AquaLab 3 TE, Decagon Devices Inc., USA). Both MC_{db} and a_w measurements were carried out on each apple cylinder.

Soluble solids content (SSC), pH and titratable acidity (TA) measurements were performed in triplicates on freeze-dried samples. SSC was measured following the method of Moscetti et al. (2018b). Briefly, 0.5 g of freeze-dried apple cylinders were mixed with 10 mL of distilled water. The resulting mixture was equilibrated, filtered and the filtrate was measured at 20 °C using a digital refractometer (mod. WM-7, Atago, Japan). Results were then converted to a fresh weight basis and expressed as °Brix (i.e., grams of sucrose per 100 g of fresh weight). Both TA and pH were measured according to Radicetti et al. (2016) with slight modifications, i.e., 1.5 g of freeze-dried sample was mixed with 100 mL of distilled water, equilibrated at 25 °C and filtered using cheesecloth. The pH was measured using a pH-meter (mod. HI 2221-02, Hanna instruments, Italy). The titration was performed using a 0.05 N NaOH solution and setting the endpoint at pH 8.1. TA was converted to a fresh mass basis to be expressed as g malic acid per 100 g of fresh mass.

2.7. Moisture prediction: regression model development

Linear regression models of the in-line changes in relative area shrinkage as a function of the relative moisture content were individually computed for each combination of pre-treatments (i.e., DS and DP). Model goodness of fit was evaluated in terms of Root Mean Square Error (RMSE), systematic error (BIAS) and adjusted coefficient of determination (adj-R^2).

2.8. Data handling and statistical analysis

Two-way analysis of variance (ANOVA) was performed to evaluate and compare the single or interaction effect of the dipping solution (DS) and the dipping pressure (DP) factors for the in-line and off-line measurements, as well as slope-intercept values and performance parameters of models. Following ANOVA, Tukey's pairwise comparison method at $P \leq 0.05$ was used to test differences between treatments or between the levels of each factor, respectively in presence or absence of a two-way interaction.

Please cite this article as: Raponi, F et al., Monitoring the hot-air drying process of organically grown apples (cv. Gala) using computer vision, *Biosystems Engineering*, https://doi.org/10.1016/j.biosystemseng.2021.07.005

Further, principal component analysis (PCA) was applied as a data fusion technique on auto-scaled (i.e., each data point was mean-centred and divided by the standard deviation) features of all in-line and off-line measurements at t_0 and t_f to evaluate between-treatment similarity. The scree-plot criterion was used to select the required number of principal components (PCs) for describing the dimensionality of the data.

Scripts for data handling, ANOVA, PCA and linear model development were prepared using R v3.4.1 in combination with 'dplyr' v0.5.0 and 'agricolae' v1.2-4 R-packages.

3. Results and discussion

3.1. *In-line measurements*

3.1.1. *Drying kinetics*

Figure 3a,b show the time courses of moisture content and drying rates, respectively, as determined by in-line monitoring of the changes in mass of the samples.

The initial dry-basis moisture content (MC_{db}) of the samples ranged from 7.01 to 8.90 g g^{-1} with the P_{50} treatments characterised by significantly higher values (Table 1), probably due to the uptake of impregnation solution (Neri et al., 2016a). The MC_{db} as calculated from the mass changes decreased irrespective of the pre-treatment following two subsequent first-order kinetics with a breakpoint at approx. 5–6 h of drying (Fig. 4). The major changes that occurred in the first 4 h of the process were in agreement with the observations made by Fernández et al. (2005) for drying of apple slices. The final MC_{db} of 0.18 g g^{-1} was reached after approximately 8 h of drying for all treatments, which was in agreement with the available literature on the drying of apple slices (Chen & Martynenko, 2013; Seiiedlou et al., 2010). For the sub-atmospheric pre-treatment, the substitution of the occluded internal gas in the open pores by the impregnation medium was observed to have no effect on the drying time.

Furthermore, the in-line measurements allowed computation of the drying rates in real-time (Fig. 3b), with precise representation of (i) the warming-up period, (ii) the first falling-rate period and (iii) the second falling-rate period. As expected, apple drying did not show a constant-rate period (Koné et al., 2013; Moscetti et al., 2018b; Zielinska et al., 2018), indicating that the water diffusion was the dominant physical mechanism of moisture movement within the apple cylinders

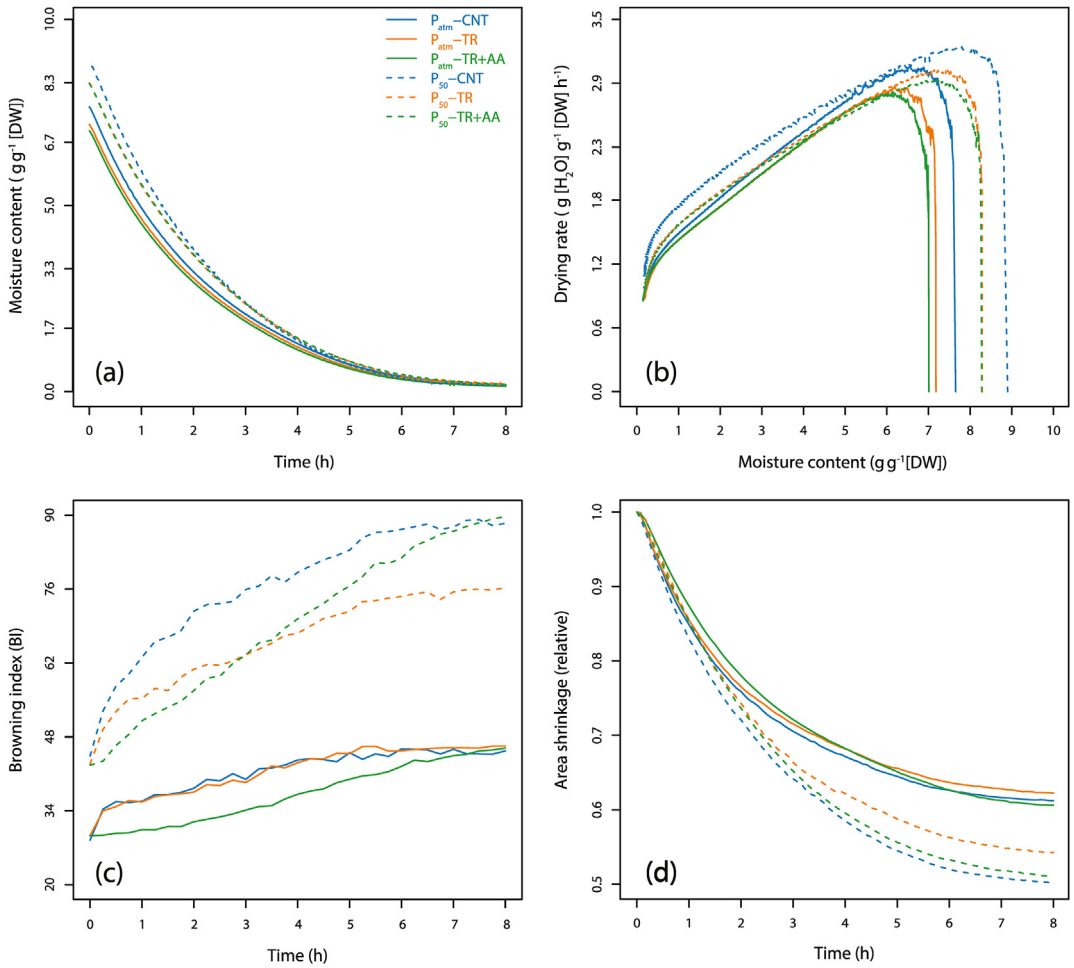

Fig. 3 – In-line monitoring of dry basis moisture content (a), drying rate (b) browning index (c) and relative area shrinkage (d) on apple cylinders subjected to various dipping treatments and dried at 60 °C up to a final dry basis moisture content of 0.18 g g^{-1}.

Please cite this article as: Raponi, F et al., Monitoring the hot-air drying process of organically grown apples (cv. Gala) using computer vision, *Biosystems Engineering*, https://doi.org/10.1016/j.biosystemseng.2021.07.005

Table 1 – The main effects of dipping solution (DS) and dipping pressure (DP) factors and the interaction of factors on the physical and chemical properties of samples at the beginning (t_0) and the end (t_f) of the drying process. Data represent sample averages calculated as a function of Dipping solution levels, Dipping pressure levels, and interaction between DS and DP factors at each combination of levels. Mean values belonging to the same group without common letters are statistically different according to Tukey's method ($P \leq 0.05$).

Factors		MC_{db} (g g^{-1} [DW])[a]		a_w[b]		SSC (°Brix)[c]		pH		TA (%)[d]		Drying rate
		t_0	t_f	t_0	t_f	t_0	t_f	t_0	t_f	t_0	t_f	(g [H_2O] g^{-1} [DW] h^{-1})
Dipping solution (DS)												
Water (CNT)		8.28	0.17	0.94 ab	0.48 a	5.70 b	74.52	4.62	4.92	1.72	1.11	1.87
Trehalose (TR)		7.73	0.20	0.95 a	0.43 c	6.16 a	71.84	4.72	4.81	1.35	1.09	1.74
Trehalose + Ascorbic Acid (TR+AA)		7.64	0.17	0.93 b	0.47 b	6.49 a	69.08	4.26	4.52	2.27	1.59	1.71
P value		ns[e]	*ns*	< 0.05	< 0.001	< 0.001	< 0.05	< 0.001	< 0.001	< 0.001	< 0.001	*ns*
Dipping condition (DP)												
Atmospheric (*Patm*)		7.28 b	0.17	0.94	0.45 b	6.63 a	71.64	4.52	4.67	1.80	1.41	1.66 b
Sub-atmospheric (P50)		8.49 a	0.19	0.94	0.47 a	5.60 b	71.99	4.55	4.83	1.76	1.11	1.88 a
P value		< 0.001	*ns*	*ns*	< 0.001	< 0.001	*ns*	*ns*	< 0.001	< 0.001	< 0.001	< 0.05
DS x DP												
CNT	*Patm*	7.65	0.18	0.94	0.47	6.09	74.58 a	4.59 c	4.79 c	1.69 d	1.28 c	1.75
CNT	P50	8.90	0.17	0.94	0.49	5.31	74.46 a	4.64 b	5.05 a	1.75 c	0.93 d	2.00
TR	*Patm*	7.18	0.18	0.95	0.43	6.72	73.40 a	4.61 bc	4.71 d	1.53 e	1.26 c	1.64
TR	P50	8.29	0.22	0.95	0.44	5.61	70.29 ab	4.83 a	4.91 b	1.17 f	0.92 d	1.83
TR+AA	*Patm*	7.01	0.15	0.93	0.46	7.10	66.94 b	4.34 d	4.52 e	2.18 b	1.70 a	1.61
TR+AA	P50	8.28	0.19	0.92	0.47	5.87	71.23 ab	4.18 e	4.52 e	2.36 a	1.49 b	1.82
P value		*ns*	*ns*	*ns*	*ns*	*ns*	< 0.05	< 0.001	< 0.001	< 0.001	< 0.001	*ns*

[a] Dry-basis moisture content.
[b] Water activity.
[c] Soluble solids content.
[d] Titratable acidity;
[e] ns, no significant differences ($P > 0.05$).

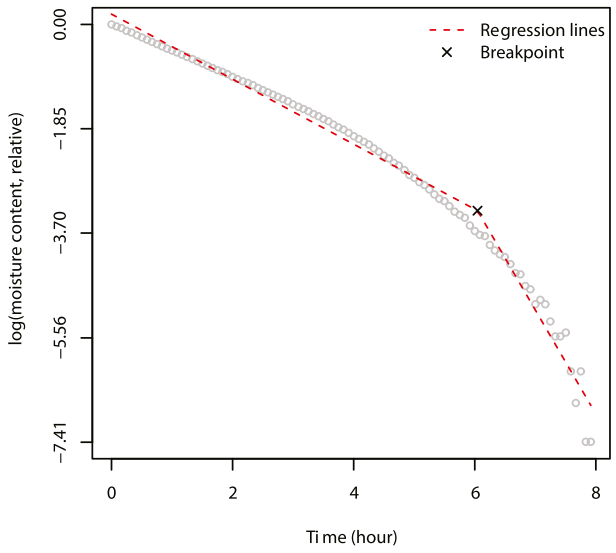

Fig. 4 – Example of segmented linear regressions representing the two subsequent first-order kinetics observed, i.e., in samples dipped in water (CNT) at atmospheric pressure (P_{atm}).

in all cases. Although dipping and pressure treatments did not affect the hygroscopic nature of apple tissue, vacuum impregnation had an impact on the desorption behaviour of apple tissues in P_{50} samples which showed the highest overall drying rate of approximately 1.88 g [H_2O] g^{-1}[DW] h^{-1} (Table 1).

3.1.2. *Colour measurements*

The 8-h drying process inevitably led to significant changes in colour, which were successfully monitored from the beginning, that is immediately after the pre-treatment (t_0), to the end (t_f) of the drying process by the CV system.

Figure 3c clearly shows the general trend of the browning index (BI) along the drying time, allowing for a rapid and intuitive 'by eye' comparison among the treatments. In general, the BI values tended to increase as the product dried which can be attributed to the well-known browning of the apple pulp. Regarding the DP factor, the P_{50} samples exhibited higher BI at t_0 compared to the P_{atm} samples. This might be due to the exposure of P_{50} samples to sub-atmospheric pressure which seemed to provoke a sudden shift in colour towards a translucent scale (i.e., a higher BI) as well as the disruption of the cell compartments causing increased interactions between the phenolic compounds and the peroxidase enzyme (Neri et al., 2016b). Subsequently, the lower L* values and higher h and C* values at t_0 of the P_{50} samples as reported in Table 2 further confirms this observation. This severe change in brightness (L*) can be attributed to the rise in the refractive index due to the physical changes in the apple tissue. This was due to the modification of gas–liquid and liquid–liquid composition of the porous apple tissues as an effect of both (i) hydrodynamic mechanisms, deformation and related phenomena induced by the sub-atmospheric pressure, and (ii) diffusion phenomena provoked by the differential in osmotic pressure between the apple matrix and the impregnation solution (Yang et al., 2017). Moreover, higher BI, lower L* and higher h and C* values were observed in P_{50} samples whereas

Table 2 – The main effects of dipping solution (DS) and dipping pressure (DP) factors and the interaction of factors on the colour and spatial data at the beginning (t_0) and the end (t_f) of the drying process. Data represent sample averages calculated as a function of Dipping solution levels, Dipping pressure levels, and interaction between DS and DP factors at each combination of levels. Mean values belonging to the same group without common letters are statistically different according to Tukey's method ($P \leq 0.05$).

Factors		Luminance (L*)		Hue angle (*h*)		Chroma (C*)		Browning index (*BI*)		Surface area (mm^2)		Eccentricity	
		t_0	t_f	t_0	t_f	t_0	t_f	t_0	t_f	t_0	t_f	t_0	t_f
Dipping solution (DS)													
Water (CNT)		68.67	67.65	75.34 c	74.60 b	19.05	30.25	36.41 a	66.90	463.45	255.54 b	0.19	0.42 a
Trehalose (TR)		69.36	68.24	76.26 b	75.11 b	19.22	28.93	36.10 ab	61.24	466.77	268.83 a	0.19	0.37 b
Trehalose + Ascorbic Acid (TR+AA)		70.15	69.52	77.66 a	78.92 a	19.50	32.05	35.95 b	67.82	465.91	261.86 ab	0.18	0.39 ab
P value		*ns*	*ns*	*< 0.001*	*< 0.001*	*ns*	*< 0.001*	*< 0.05*	*< 0.001*	*ns*	*< 0.001*	*ns*	*< 0.001*
Dipping condition (DP)													
Atmospheric (*Patm*)		72.68 a	71.67 a	73.63 b	74.73 b	16.54 b	24.41	29.00 b	45.85	454.55 b	280.97 a	0.18	0.32 b
Sub-atmospheric (*P50*)		66.11 b	65.27 b	79.20 a	77.69 a	21.97 a	36.41	43.31 a	84.79	476.20 a	243.18 b	0.19	0.47 a
P value		*< 0.001*	*< 0.001*	*< 0.001*	*< 0.001*	*< 0.001*	*< 0.001*	*< 0.001*	*< 0.001*	*< 0.001*	*< 0.001*	*ns*	*< 0.001*
DS x DP													
CNT	*Patm*	72.43	71.42	72.72	73.49	16.20	24.02 c	28.43	45.36 c	453.24	278.96	0.19	0.33
CNT	*P50*	64.91	63.89	77.95	75.71	21.90	36.49 a	44.39	88.44 a	473.67	232.12	0.19	0.51
TR	*Patm*	71.86	70.57	73.63	73.26	16.42	23.91 c	29.30	46.28 c	453.26	283.65	0.19	0.31
TR	*P50*	66.85	65.91	78.89	76.96	22.02	33.95 b	42.90	76.20 b	480.27	254.01	0.19	0.43
TR+AA	*Patm*	73.73	73.01	74.54	77.44	16.99	25.30 c	29.26	45.90 c	457.16	280.31	0.18	0.31
TR+AA	*P50*	66.58	66.02	80.77	80.40	22.00	38.80 a	42.64	89.73 a	474.67	243.41	0.19	0.46
P value		*ns*	*ns*	*ns*	*ns*	*ns*	*< 0.05*	*ns*	*< 0.05*	*ns*	*ns*	*ns*	*ns*

[a] ns, no significant differences ($P > 0.05$).

P_{atm} samples maintained relatively lower BI, higher L* and lower h and C* values after drying (t_f).

As for the dipping solutions (DS), Fig. 3c gives a general idea of efficacy of the treatments, with the use of different solutions, i.e., TR and TR+AA, slowing down the browning development. This is particularly evident in case of P_{50} samples with TR partially hindering the browning development during the whole process by inhibiting the enzymatic changes as also observed by Neri et al. (2016) in sliced, fresh-like apple products. The use of TR+AA solution was effective against browning for only up to 6-h drying in P_{50} and P_{atm} samples, probably due to the fact that AA is a competitive inhibitor and its conversion to dehydroascorbic acid further increases the browning (Altunkaya & Gökmen, 2008). To further elucidate, the DS significantly affected the hue angle (h) of the final products (Table 2), with TR+AA resulting in higher values tending towards yellowish hues in comparison to CNT and TR pre-treated samples. This change in hue might be attributed to the browning pigments developed during drying. As for the chroma (C*), the values were influenced by the interaction of DS and DP factors, with CNT and TR+AA particularly in combination with P_{50} pressure resulted in higher colour saturation than the corresponding P_{atm} samples. These differences in C* values were confirmed by the higher h and BI values in P_{50} samples owing to the physico-chemical changes in the apple tissue.

3.1.3. *Spatial measurements*

Figure 3d shows the general tendency of the relative area shrinkage of the samples along the drying time, which decreases in a similar fashion to that of moisture content (Fig. 3a). Within the DP factor, P_{50} samples showed a higher development of area shrinkage, whereas for the DS factor, use of trehalose registered a gradual and relatively lower decrease in the shrinkage values along the drying time. The values for surface area (mm^2) as presented in Table 2, further confirm this observation. In addition, the P_{50} samples registered significantly higher values at t_0 and lower values at t_f than P_{atm} samples, probably due to higher shrinkage rates. The higher surface area observed in P_{50} samples at t_0 can be attributed to the swelling and volumetric increase in size of the cells due to the hydro-dynamic relaxation phenomenon and inflow of the impregnation solution (Neri et al., 2016a). Subsequently, the removal of moisture resulted in significant loss of the surface area at t_f occupied by the apple tissue. In fact, vacuum impregnation is well-known for its capability in modifying the physical properties of a tissue and affecting further processing (Fito et al., 2001).

As for DS, although no significant effect was noticed at t_0, the dried samples evidently were affected by presence of TR. Dipping in TR lowered the area shrinkage, resulting in significantly higher surface area (Table 2) which can be related to a case hardening effect, as already observed by Aktas et al. (2007) during drying of potato and carrot slices pre-treated with trehalose. For all the pre-treatments investigated the perimeter values showed the same trend observed for the surface area but were noisy (data not shown) and hence were not used for further model development.

The minor and major axes values were observed to decrease in general from t_0 to t_f describing well the change in the sample size as a consequence of moisture loss. As such, the minor axis values decreased from an average of 24.10 to 17.10 mm, whereas the major axis decreased from an average of 24.59 to 19.22 mm. Thus, the eccentricity values increased from an average of 0.19–0.39 (Table 2) and were affected significantly at t_f by DS and DP factors. These observations

Please cite this article as: Raponi, F et al., Monitoring the hot-air drying process of organically grown apples (cv. Gala) using computer vision, *Biosystems Engineering*, https://doi.org/10.1016/j.biosystemseng.2021.07.005

were in accordance with the surface area and shrinkage changes, confirming an elliptical shape development during drying.

The results highlighted few trends: (i) the eccentricity of samples increased along the drying time with the loss of surface area in all samples; (ii) P_{50} samples were more elliptical than P_{atm} samples due to the cellular deformation; (iii) dipping in TR resulted in the lowest eccentricity values, i.e., roundest samples.

3.2. *Off-line measurements: physicochemical changes*

The main effects of dipping solution (DS), dipping pressure (DP) and their interaction (DS x DP) on the physico-chemical changes that influence the stability and final quality of apple samples were evaluated at times t_0 and t_f and are reported in Table 1.

In general, MC_{db}, a_w and TA decreased during drying whereas the pH and SSC increased as expected. The MC_{db}, as already noted, was not affected by any of the tested factors at the initial or final drying times, except for the factor DP at t_0. Further, as observed in drying rates, fresh P_{50} samples resulted in significantly higher values of initial moisture content due to the uptake of impregnation solution by the apple tissues (Neri et al., 2016b). The water activity value reduced from 0.93 to 0.95 (t_0) to 0.43–0.48 in the dried samples (t_f) and was influenced by both DS and DP. For the DS, lowest a_w values at t_f were observed in TR treated samples followed by TR+AA due to the uptake of solutes (Tylewicz et al., 2019). As for the DP, although no differences in a_w were noticeable at t_0, the values were significantly higher in P_{50} samples at t_f but were noted to be of no practical consequences in terms of absolute values (Neri et al., 2016b).

Regarding the SSC, as expected the values increased with drying time due to the removal of the moisture and were significantly affected by the interaction of the other considered factors. As for the samples at t_0, the use of TR and AA slightly increased SSC due to the uptake of solutes whereas the use of sub-atmospheric pressure slightly decreased it. These lower SSC values in P_{50} samples is due to the loss of native solids caused by the outflow of native cellular fluid caused by internal gas expansion which was probably only partially replaced by the solutes owing to the low concentrations (Gras et al., 2002; Tylewicz et al., 2019).

As for the pH and TA, the values at both t_0 and t_f were influenced by the interaction of the factors considered. The pH tended to be higher with P_{50} samples compared to P_{atm} samples due to the uptake of impregnating liquids that tend to be alkaline in nature, particularly in case of TR. Whereas, in TR+AA treated samples the pH tended to decrease evidently due to the acidifying nature of AA with P_{50} samples registering lowest values due to the impregnation effect (Assis et al., 2019). Furthermore, the higher TA in TR+AA treated samples at both t_0 and t_f further confirmed the uptake of ascorbic acid during dipping treatments.

To summarise the off-line measurements, the physicochemical changes were observed to be influenced by both the DS and DP used at t_0 as well as t_f which allows us to hypothesise that these changes might be reflected in the in-line measurements thereby influencing the number of prediction models required.

3.3. *Overview of the data using the principal component analysis (PCA)*

Principal component analysis was carried out to provide an overview of the effect of dipping solutions and dipping pressures at the two drying stages (t_0 and t_f) on ample performance. It can be seen from the biplot (Fig. 5), that the samples were clearly split into four clusters within the two-dimensional spaces defined by PC1 and PC2 and accounted for 72.40% and 15.58% of variance, respectively, equal to a total of 87.98%. PC1 was observed to clearly cluster in the samples according to drying time, whilst PC2 allowed dipping pressures to be visually discriminated. In detail, fresh samples (t_0) were in the II and III quadrants (P_{atm} and P_{50}, respectively) and dried samples (t_f) were positioned in the I and IV quadrants (P_{atm} and P_{50}, respectively). Each cluster was composed of the three dipping solution levels and no clear patterns for the dipping solution factor were evidenced.

Concerning the in-line measurements, spatial and colour parameters contributed to both PCs, except for luminance and chroma. In fact, the loadings of L* and C* showed their major contribution in arranging samples along the PC2 and, thus, the dipping pressure used. The other colour parameters had positive loadings correlated to PC1 and were thus closely associated to drying time. Only the redness (a*) was positively correlated with PC2, while the browning index (BI), yellowness (b*) and hue angle (h) had negative loadings and were clustered together. Regarding the morphological parameters, PC1 was positively correlated only with the eccentricity, while PC2 had negative correlations with all of them. In fact, only eccentricity increased during drying, and all morphological changes were less pronounced in P_{atm} samples.

For the off-line measurements, MC_{db}, a_w, SSC, TA and pH contributed to both of the PCs. For SSC, pH parameters were observed to contribute positively whereas MC_{db}, TA and a_w

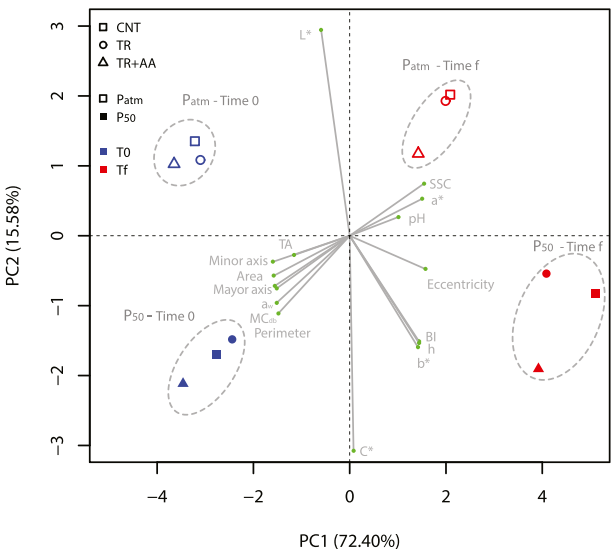

Fig. 5 – Principal component analysis of data variations (impact of treatments and drying process) on apple cylinders. Biplot of the scores and the loadings are represented for PC1 vs PC2.

contributed negatively to both PC1 and PC2. This can be explained by the increase in SSC and pH in the dried samples positioning these parameters in I quadrant. The other off-line parameters decreased along the drying time and were thus in the III quadrant. The positioning of these parameters in correlation to P_{atm} and P_{50} samples can be attributed to the influence of dipping pressures and their subsequent effects as observed in Table 1.

3.4. CV-based prediction models of moisture content

Based on the simultaneous and perceivable changes in moisture content, and the relative area shrinkage of the samples at times t_0 and t_f, it was hypothesised that shrinkage could be used as a predictor of moisture changes in the apple tissue. Subsequently, linear regression models for moisture content predicted from area shrinkage were developed as shown in Fig. 6a. The regression coefficients and performance metrics for the developed models are summarised in Table 3.

The results show that the models have excellent prediction capability for all the pre-treatment pressures investigated, with adjusted R^2 values always greater than 99.80%. As for the RMSE and BIAS the values were lower than 0.040 and 8.5×10^{-3}, respectively and were not affected by the processing factors. Further, as hypothesised in the previous discussion among the DS and DP factors, the different DS (CNT, TR, TR+AA) were not found to influence the prediction models. However, the regression coefficients, i.e., the intercept and slope, as affected by the DP factor indicated a significant effect of dipping pressure necessitating two linear models for moisture prediction (Table 3). Thus, one model for each dipping pressure was developed as presented also in Fig. 6a, wherein P_{50} samples exhibited a higher slope which can be related to the higher drying rates and sharp decrease in the relative area shrinkage as already observed during the first 4 h of drying. Further, Fig. 6b shows that the relative area shrinkage is a good predictor of moisture irrespective of the dipping solutions with no observable under and/or over-fitting for both the dipping pressures used. Also, plots Fig. 6c,d confirm the predicted moisture changes along the drying time for P_{atm} and P_{50} samples, respectively. Several authors reported the feasibility of utilising computer vision in combination with artificial neural networks to predict moisture changes in the product during processing (Behroozi Khazaei et al., 2013; Nadian et al., 2015). However, the models presented in this study demonstrate that simple linear regression can assure excellent prediction of moisture change by using only the area shrinkage of the differently pre-treated apple samples.

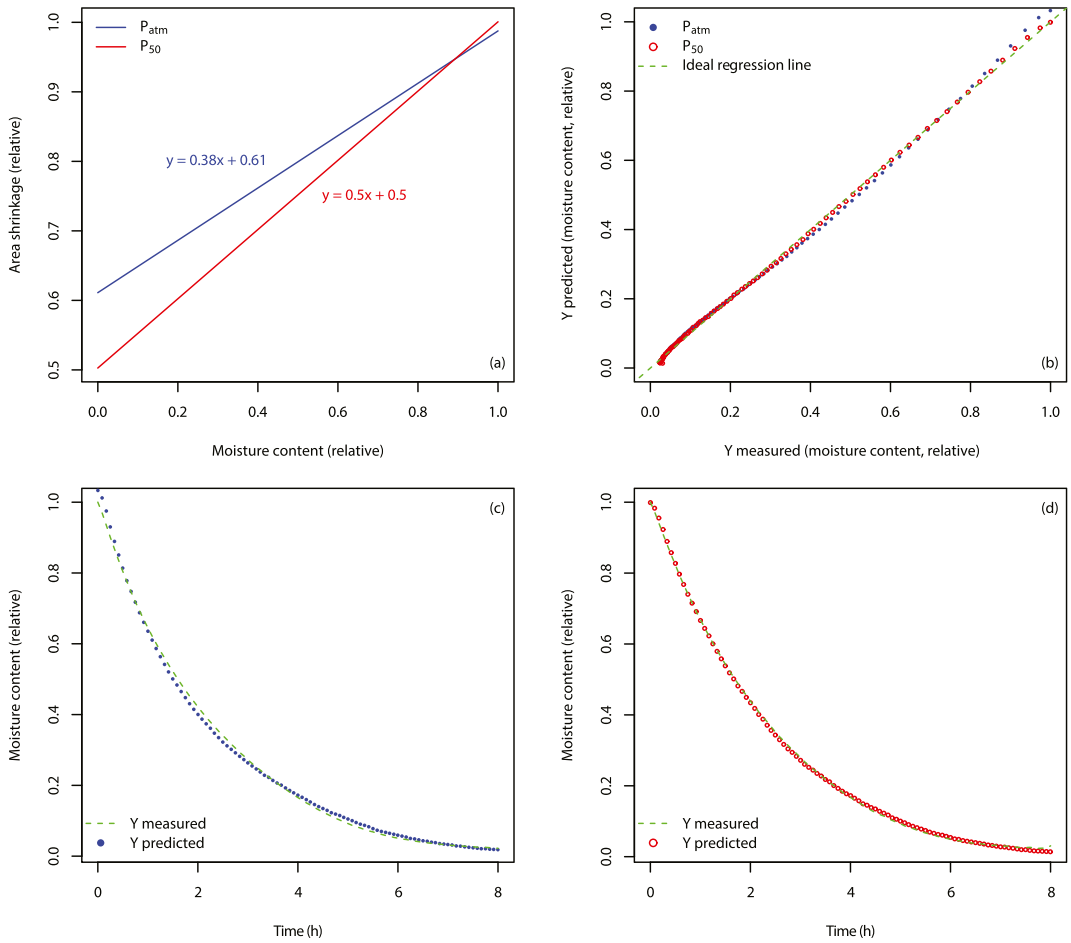

Fig. 6 – Regression models of relative moisture content vs. relative area shrinkage as a function of dipping pressure (P_{atm}, blue line, closed symbol; P_{50}, red line, open symbol): linear regression models (a), predicted vs. measured plot (b), and predicted and measured moisture content vs. time plots (c and d).

Please cite this article as: Raponi, F et al., Monitoring the hot-air drying process of organically grown apples (cv. Gala) using computer vision, *Biosystems Engineering*, https://doi.org/10.1016/j.biosystemseng.2021.07.005

Table 3 – The main effects of dipping solution (DS) and dipping pressure (DP) factors and the interaction of factors on the regression coefficients and performance metrics of the moisture content vs. area shrinkage models. Data represent parameter estimate averages calculated as a function of Dipping solution levels, Dipping pressure levels, and interaction between DS and DP factors at each combination of levels. Mean values belonging to the same group without common letters are statistically different according to Tukey's method ($P \leq 0.05$).

Factors		Regression coefficients		Performance metrics		
		Intercept	Slope	RMSE	BIAS	Adj-R^2 (%)
Dipping solution (DS)						
Water (CNT)		0.54	0.44	0.030	−2.31E-02	99.86
Trehalose (TR)		0.57	0.42	0.027	1.88E-02	99.87
Trehalose + Ascorbic Acid (TR+AA)		0.56	0.45	0.015	4.37E-03	99.94
P value		*ns*[a]	*ns*	*ns*	*ns*	*ns*
Dipping condition (DP)						
Atmospheric (P_{atm})		0.61 a	0.38 b	0.021	1.34E-04	99.84 b
Sub-atmospheric (P_{50})		0.50 b	0.50 a	0.028	−1.42E-04	99.95 a
P value		*< 0.001*	*< 0.001*	*ns*	*ns*	*< 0.001*
DS x DP						
CNT	P_{atm}	0.61	0.37	0.022	−1.19E-02	99.79
CNT	P_{50}	0.48	0.51	0.039	1.20E-02	99.82
TR	P_{atm}	0.62	0.36	0.021	2.97E-04	99.90
TR	P_{50}	0.52	0.48	0.032	−3.44E-02	99.94
TR+AA	P_{atm}	0.61	0.39	0.019	2.55E-02	99.92
TR+AA	P_{50}	0.51	0.50	0.012	8.44E-03	99.97
P value		*ns*	*ns*	*ns*	*ns*	*ns*

[a] ns, no significant differences ($P > 0.05$).

4. Conclusions

A CV based smart-enabled prototype dryer with potential for scale-up and industrial applications was evaluated to non-destructively monitor real-time quality changes in differently pre-treated apple cylinders (*M. domestica* B. var. Gala). The results of the study show that CV can be effectively used as a PAT tool for process monitoring and control of apple to drying using the identified quality parameters (i.e., shape and size, moisture content and colour). The results show that the upper digital images of the apple cylinders can effectively be used to monitor, describe, and distinguish the product morphological changes within a drying process, indicating that the system is flexible for different applications. Subsequently, the linear models were developed based only on area shrinkage for moisture content showed excellent prediction results ($R^2 > 0.98$) for all the pre-treatments investigated. The system was robust to dipping solutions (CNT, TR, and TR+AA) whereas differences between the different dipping pressures (P_{atm} and P_{50}) used thereby resulting in two linear models for moisture prediction. Finally, the approach utilised in this study represents a potential step towards a scalable low-cost, smart enabled CV-based dryer for real-time monitoring of the product drying. This could be further improved by integrating a systematic Quality-by-Design approach that can positively impact process sustainability through implementation of deep chemometrics using both spatial and spectral domains. In addition, further investigation on multiple sample layers, other fruits and vegetables, and process parameters not covered by the present study could yield improved information on the transferability and robustness of the developed solution.

Authorship conformation

Please check the following as appropriate:

All authors have participated in (a) conception and design, or analysis and interpretation of the data; (b) drafting the article or revising it critically for important intellectual content; and (c) approval of the final version.

This manuscript has not been submitted to, nor is under review at, another journal or other publishing venue.

The authors have no affiliation with any organization with a direct or indirect financial interest in the subject matter discussed in the manuscript.

Declaration of competing interest

The authors declare that they have no known competing financial interests or personal relationships that could have appeared to influence the work reported in this paper.

Acknowledgments

The authors gratefully acknowledge [1] CORE Organic Plus consortium (ERA-NET action) and Mipaaf (Ministero delle politiche agricole alimentari e forestali - Italy) for financial support through the SusOrgPlus project (D.M. 20/12/2017, n. 92350) and [2] the 'Departments of excellence 2018' program (i.e. 'Dipartimenti di eccellenza') of the Italian Ministry of Education, University and Research for the financial support through the 'Landscape 4.0 food, wellbeing and environment' (DIBAF department of University of Tuscia). Moreover, our

sincere thanks to the master student Serena Santopadre and to the bachelor student Giordana Ventriglia for their valuable help and support during the experimentation.

REFERENCES

Aghbashlo, M., Hosseinpour, S., & Ghasemi-Varnamkhasti, M. (2014). Computer vision technology for real-time food quality assurance during drying process. *Trends in Food Science & Technology, 39*(Issue 1), 76–84. https://doi.org/10.1016/j.tifs.2014.06.003. Elsevier Ltd.

Aktas, T., Fujii, S., Kawano, Y., & Yamamoto, S. (2007). Effects of pretreatments of sliced vegetables with trehalose on drying characteristics and quality of dried products. *Food and Bioproducts Processing, 85*(3 C), 178–183. https://doi.org/10.1205/fbp07037

Albanese, D., Cinquanta, L., & Di Matteo, M. (2007). Effects of an innovative dipping treatment on the cold storage of minimally processed Annurca apples. *Food Chemistry, 105*(3), 1054–1060. https://doi.org/10.1016/j.foodchem.2007.05.009

Altunkaya, A., & Gökmen, V. (2008). Effect of various inhibitors on enzymatic browning, antioxidant activity and total phenol content of fresh lettuce (Lactuca sativa). *Food Chemistry, 107*(3), 1173–1179. https://doi.org/10.1016/j.foodchem.2007.09.046

Assis, F. R., Rodrigues, L. G. G., Tribuzi, G., de Souza, P. G., Carciofi, B. A. M., & Laurindo, J. B. (2019). Fortified apple (Malus spp., var. Fuji) snacks by vacuum impregnation of calcium lactate and convective drying. *LWT, 113*, 108298. https://doi.org/10.1016/j.lwt.2019.108298

Barbosa de Lima, A. G., Da Silva, J. V., Pereira, E. M. A., Dos Santos, I. B., & Barbosa de Lima, W. M. P. (2015). Drying of bioproducts: Quality and energy aspects. In *Drying and energy technologies* (pp. 1–18). Springer International Publishing. https://doi.org/10.1007/978-3-319-19767-8_1.

Basunia, M. A., & Abe, T. (2001). Thin-layer solar drying characteristics of rough rice under natural convection. *Journal of Food Engineering, 47*(4), 295–301. https://doi.org/10.1016/S0260-8774(00)00133-3

Behroozi Khazaei, N., Tavakoli, T., Ghassemian, H., Khoshtaghaza, M. H., & Banakar, A. (2013). Applied machine vision and artificial neural network for modeling and controlling of the grape drying process. *Computers and Electronics in Agriculture, 98*, 205–213. https://doi.org/10.1016/j.compag.2013.08.010

Chen, Y., & Martynenko, A. (2013). Computer vision for real-time measurements of Shrinkage and color changes in blueberry convective drying. *Drying Technology, 31*(10), 1114–1123. https://doi.org/10.1080/07373937.2013.775587

Defraeye, T. (2014). Advanced computational modelling for drying processes - a review. *Applied Energy, 131*, 323–344. https://doi.org/10.1016/j.apenergy.2014.06.027. Elsevier Ltd.

El-Sebaii, A. A., & Shalaby, S. M. (2012). Solar drying of agricultural products: A review. *Renewable and Sustainable Energy Reviews, 16*(Issue 1), 37–43. https://doi.org/10.1016/j.rser.2011.07.134. Elsevier Ltd.

El-Shimi, N. M. (1993). Control of enzymatic browning in apple slices by using ascorbic acid under different conditions. *Plant Foods for Human Nutrition, 43*(1), 71–76. https://doi.org/10.1007/BF01088098

Fernández, L., Castillero, C., & Aguilera, J. M. (2005). An application of image analysis to dehydration of apple discs. *Journal of Food Engineering, 67*(1–2), 185–193. https://doi.org/10.1016/j.jfoodeng.2004.05.070

Fito, P., Chiralt, A., Barat, J. M., Andrés, A., Martínez-Monzó, J., & Martínez-Navarrete, N. (2001). Vacuum impregnation for development of new dehydrated products. *Journal of Food Engineering, 49*(4), 297–302. https://doi.org/10.1016/S0260-8774(00)00226-0

Gras, M., Vidal-Brotóns, N., Betoret, A., Chiralt, & Fito, P. (2002). The response of some vegetables to vacuum impregnation. *Innovative Food Science & Emerging Technologies, 3*(3), 263–269. https://doi.org/10.1016/S1466-8564(02)00032-2

Janssen, M. (2018). Determinants of organic food purchases: Evidence from household panel data. *Food Quality and Preference, 68*(February), 19–28. https://doi.org/10.1016/j.foodqual.2018.02.002

Kearney, J. (2010). Food consumption trends and drivers. *Philosophical Transactions of the Royal Society B: Biological Sciences, 365*(1554), 2793–2807. https://doi.org/10.1098/rstb.2010.0149

Kemp, I. C. (2005). Reducing dryer energy use by process integration and pinch analysis. *Drying Technology, 23*(9–11), 2089–2104. https://doi.org/10.1080/07373930500210572

Koné, K. Y., Druon, C., Gnimpieba, E. Z., Delmotte, M., Duquenoy, A., & Laguerre, J. C. (2013). Power density control in microwave assisted air drying to improve quality of food. *Journal of Food Engineering, 119*(4), 750–757. https://doi.org/10.1016/j.jfoodeng.2013.06.044

Koyuncu, T. (2006). Performance of various design of solar air heaters for crop drying applications. *Renewable Energy, 31*(7), 1073–1088. https://doi.org/10.1016/j.renene.2005.05.017

Lawless, H. T. (1999). *Color and appearance* (pp. 406–429). https://doi.org/10.1007/978-1-4615-7843-7_12

Lukinac, J., Velić, D., Magdić, D., Mujić, I., Bilić, M., & Jokić, S. (2013). Antibrowning effects of various pretreatment methods on dried apple samples. *Acta Horticulturae, 989*, 261–270. https://doi.org/10.17660/ActaHortic.2013.989.34

Maltini, E., Torreggiani, D., Venir, E., & Bertolo, G. (2003). Water activity and the preservation of plant foods. *Food Chemistry, 82*(1), 79–86. https://doi.org/10.1016/S0308-8146(02)00581-2

Megarry, A. J., Booth, J., & Burley, J. (2011). Amorphous trehalose dihydrate by cryogenic milling. *Carbohydrate Research, 346*(8), 1061–1064. https://doi.org/10.1016/J.CARRES.2011.03.011

Moscetti, R., Carletti, L., Monarca, D., Cecchini, M., Stella, E., & Massantini, R. (2013). Effect of alternative postharvest control treatments on the storability of 'Golden Delicious' apples. *Journal of the Science of Food and Agriculture, 93*(11), 2691–2697. https://doi.org/10.1002/jsfa.6086

Moscetti, R., Haff, R. P., Ferri, S., Raponi, F., Monarca, D., Liang, P., & Massantini, R. (2017). Real-time monitoring of organic carrot (var. Romance) during hot-air drying using near-infrared spectroscopy. *Food and Bioprocess Technology, 10*(11), 2046–2059. https://doi.org/10.1007/s11947-017-1975-3

Moscetti, R., Massantini, R., & Fidaleo, M. (2019). Application on-line NIR spectroscopy and other process analytical technology tools to the characterization of soy sauce desalting by electrodialysis. *Journal of Food Engineering, 263*, 243–252. https://doi.org/10.1016/j.jfoodeng.2019.06.022

Moscetti, R., Raponi, F., Ferri, S., Colantoni, A., Monarca, D., & Massantini, R. (2018a). Real-time monitoring of organic apple (var. Gala) during hot-air drying using near-infrared spectroscopy. *Journal of Food Engineering, 222*, 139–150. https://doi.org/10.1016/j.jfoodeng.2017.11.023

Moscetti, R., Raponi, F., Ferri, S., Colantoni, A., Monarca, D., & Massantini, R. (2018b). Real-time monitoring of organic apple (var. Gala) during hot-air drying using near-infrared spectroscopy. *Journal of Food Engineering, 222*, 139–150. https://doi.org/10.1016/j.jfoodeng.2017.11.023

Moscetti, R., Sturm, B., Crichton, S. O. J., Amjad, W., & Massantini, R. (2018). Postharvest monitoring of organic potato (cv. Anuschka) during hot-air drying using visible–NIR hyperspectral imaging. *Journal of the Science of Food and Agriculture*. https://doi.org/10.1002/jsfa.8737

Mujumdar, A. S., & Law, C. L. (2010). Drying technology: Trends and applications in postharvest processing. *Food and Bioprocess*

Technology, 3(6), 843–852. https://doi.org/10.1007/s11947-010-0353-1

Nadian, M. H., Rafiee, S., Aghbashlo, M., Hosseinpour, S., & Mohtasebi, S. S. (2015). Continuous real-time monitoring and neural network modeling of apple slices color changes during hot air drying. *Food and Bioproducts Processing, 94*, 263–274. https://doi.org/10.1016/j.fbp.2014.03.005

Neri, L., Di Biase, L., Sacchetti, G., Di Mattia, C., Santarelli, V., Mastrocola, D., & Pittia, P. (2016a). Use of vacuum impregnation for the production of high quality fresh-like apple products. *Journal of Food Engineering, 179*, 98–108. https://doi.org/10.1016/j.jfoodeng.2016.02.002

Neri, L., Di Biase, L., Sacchetti, G., Di Mattia, C., Santarelli, V., Mastrocola, D., & Pittia, P. (2016b). Use of vacuum impregnation for the production of high quality fresh-like apple products. *Journal of Food Engineering, 179*, 98–108. https://doi.org/10.1016/j.jfoodeng.2016.02.002

Ngamwonglumlert, L., & Devahastin, S. (2017). Microstructure and its relationship with quality and storage stability of dried foods. In *Food microstructure and its relationship with quality and stability* (pp. 139–159). Elsevier. https://doi.org/10.1016/B978-0-08-100764-8.00008-3.

Pathare, P. B., Opara, U. L., & Al-Said, F. A.-J. (2013). Colour measurement and analysis in fresh and processed foods: A review. *Food and Bioprocess Technology, 6*(1), 36–60. https://doi.org/10.1007/s11947-012-0867-9

Perez, F., & Granger, B. E. (2015). *Project Jupyter: Computational narratives as the engine of collaborative data science*. https://blog.jupyter.org.

Pomerantsev, A. L., & Ye, O. (2012). *Process analytical technology: A critical view of the chemometricians*. https://doi.org/10.1002/cem.2445

Radicetti, E., Massantini, R., Campiglia, E., Mancinelli, R., Ferri, S., & Moscetti, R. (2016). Yield and quality of eggplant (Solanum melongena L.) as affected by cover crop species and residue management. *Scientia Horticulturae, 204*, 161–171. https://doi.org/10.1016/j.scienta.2016.04.005

Raponi, F., Moscetti, R., Monarca, D., Colantoni, A., & Massantini, R. (2017). Monitoring and optimization of the process of drying fruits and vegetables using computer vision: A review. *Sustainability (Switzerland), 9*(11). https://doi.org/10.3390/su9112009

Sacilik, K., & Elicin, A. K. (2006). The thin layer drying characteristics of organic apple slices. *Journal of Food Engineering, 73*(3), 281–289. https://doi.org/10.1016/j.jfoodeng.2005.03.024

Sampson, D. J., Chang, Y. K., Rupasinghe, H. P. V., & Zaman, Q. U. (2014). A dual-view computer-vision system for volume and image texture analysis in multiple apple slices drying. *Journal of Food Engineering, 127*, 49–57. https://doi.org/10.1016/j.jfoodeng.2013.11.016

Seiiedlou, S., Ghasemzadeh, H. R., Hamdami, N., Talati, F., & Moghaddam, M. (2010). Convective drying of apple: Mathematical modeling and determination of some quality parameters. *International Journal of Agriculture and Biology, 12*(2), 171–178. https://doi.org/10.1063/1.1527694

Simal, S., Deyá, E., Frau, M., & Rosselló, C. (1997). Simple modelling of air drying curves of fresh and osmotically pre-dehydrated apple cubes. *Journal of Food Engineering, 33*(1–2), 139–150. https://doi.org/10.1016/s0260-8774(97)00049-6

Singh, D. B., Ahmed, N., Pal, A. A., Kumar, R., & Mirza, A. A. (2015). Effect of anti browning agents and slice thickness on drying and quality of apple slices var. Red Chief. *Journal of Applied Horticulture, 17*(1), 48–51. https://doi.org/10.37855/jah.2015.v17i01.10

Sun, Q., Zhang, M., & Mujumdar, A. S. (2018). Recent developments of artificial intelligence in drying of fresh food: A review. *Critical Reviews in Food Science and Nutrition, 1*–65. https://doi.org/10.1080/10408398.2018.1446900

Su, Y., Zhang, M., & Mujumdar, A. S. (2015). Recent developments in smart drying technology. *Drying Technology, 33*(3), 260–276. https://doi.org/10.1080/07373937.2014.985382. Taylor and Francis Inc.

Tunde-Akintunde, T. Y. (2011). Mathematical modeling of sun and solar drying of chilli pepper. *Renewable Energy, 36*(8), 2139–2145. https://doi.org/10.1016/j.renene.2011.01.017

Tylewicz, U., Mannozzi, C., Romani, S., Castagnini, J. M., Samborska, K., Rocculi, P., & Dalla Rosa, M. (2019). Chemical and physicochemical properties of semi-dried organic strawberries enriched with bilberry juice-based solution. *LWT, 114*, 108377. https://doi.org/10.1016/j.lwt.2019.108377

van den Berg, F., Lyndgaard, C. B., Sørensen, K. M., & Engelsen, S. B. (2013). Process analytical technology in the food industry. *Trends in Food Science & Technology, 31*(Issue 1), 27–35. https://doi.org/10.1016/j.tifs.2012.04.007. Elsevier.

Vega-Gálvez, A., Ah-Hen, K., Chacana, M., Vergara, J., Martínez-Monzó, J., García-Segovia, P., Lemus-Mondaca, R., & Di Scala, K. (2012). Effect of temperature and air velocity on drying kinetics, antioxidant capacity, total phenolic content, colour, texture and microstructure of apple (var. Granny Smith) slices. *Food Chemistry, 132*(1), 51–59. https://doi.org/10.1016/j.foodchem.2011.10.029

Velić, D., Planinić, M., Tomas, S., & Bilić, M. (2004). Influence of airflow velocity on kinetics of convection apple drying. *Journal of Food Engineering, 64*(1), 97–102. https://doi.org/10.1016/j.jfoodeng.2003.09.016

Winiczenko, R., Górnicki, K., Kaleta, A., Martynenko, A., Janaszek-Mańkowska, M., & Trajer, J. (2018). Multi-objective optimization of convective drying of apple cubes. *Computers and Electronics in Agriculture, 145*, 341–348. https://doi.org/10.1016/J.COMPAG.2018.01.006

Xu, F., Jin, X., Zhang, L., & Chen, X. D. (2017). Investigation on water status and distribution in broccoli and the effects of drying on water status using NMR and MRI methods. *Food Research International*. https://doi.org/10.1016/j.foodres.2017.03.041

Yang, H., Wu, Q., Ng, L. Y., & Wang, S. (2017). Effects of vacuum impregnation with calcium lactate and pectin methylesterase on quality attributes and chelate-soluble pectin morphology of fresh-cut papayas. *Food and Bioprocess Technology, 10*(5), 901–913. https://doi.org/10.1007/s11947-017-1874-7

Yaseen, T., Sun, D.-W., & Cheng, J.-H. (2017). Raman imaging for food quality and safety evaluation: Fundamentals and applications. *Trends in Food Science & Technology, 62*, 177–189. https://doi.org/10.1016/J.TIFS.2017.01.012

Zielinska, M., Zielinska, D., & Markowski, M. (2018). The effect of microwave-vacuum pretreatment on the drying kinetics, color and the content of bioactive compounds in osmo-microwave-vacuum dried cranberries (Vaccinium macrocarpon). *Food and Bioprocess Technology, 11*(3), 585–602. https://doi.org/10.1007/s11947-017-2034-9

Please cite this article as: Raponi, F et al., Monitoring the hot-air drying process of organically grown apples (cv. Gala) using computer vision, *Biosystems Engineering*, https://doi.org/10.1016/j.biosystemseng.2021.07.005